ISSN 1674-1056
http://cpb.iphy.ac.cn
http://iopscience.iop.org/cpb
中国物理 B
Chinese Physics
中国物理 Chinese Physics B

Pressure-induced enhancement of optoelectronic properties in PtS_2

Yi-Fang Yuan(袁亦方), Zhi-Tao Zhang(张志涛), Wei-Ke Wang(王伟科), Yong-Hui Zhou(周永惠), Xu-Liang Chen(陈绪亮), Chao An(安超), Ran-Ran Zhang(张冉冉), Ying Zhou(周颖), Chuan-Chuan Gu(顾川川), Liang Li(李亮), Xin-Jian Li(李新建), Zhao-Rong Yang(杨昭荣)
Citation: Chin. Phys. B . 2018, 27(6): 066201. **doi:** 10.1088/1674-1056/27/6/066201

Journal homepage: http://cpb.iphy.ac.cn; http://iopscience.iop.org/cpb

What follows is a list of articles you may be interested in

Neutron powder diffraction and high-pressure synchrotron x-ray diffraction study of tantalum nitrides

Lei-hao Feng(冯雷豪), Qi-wei Hu(胡启威), Li Lei(雷力), Lei-ming Fang(房雷鸣), Lei Qi(戚磊), Lei-lei Zhang(张雷雷), Mei-fang Pu(蒲梅芳), Zi-li Kou(寇自力), Fang Peng(彭放), Xi-ping Chen(陈喜平), Yuan-hua Xia(夏元华), Yohei Kojima(小岛洋平), Hiroaki Ohfuji(大藤宏明), Duan-wei He(贺端威), Bo Chen(陈波), Tetsuo Irifune(入舩徹男)
Chin. Phys. B . 2018, 27(2): 026201. **doi:** 10.1088/1674-1056/27/2/026201

Exploring the compression behavior of HP-$BiNbO_4$ under high pressure

Yin-Juan Liu(刘银娟), Jia-Wei Zhang(张佳威), Duan-Wei He(贺端威), Chao Xu(许超), Qi-Wei Hu(胡启威), Lei Qi(戚磊), A-Kun Liang(梁阿坤)
Chin. Phys. B . 2017, 26(11): 116202. **doi:** 10.1088/1674-1056/26/11/116202

How to detect melting in laser heating diamond anvil cell

Liuxiang Yang(杨留响)
Chin. Phys. B . 2016, 25(7): 076201. **doi:** 10.1088/1674-1056/25/7/076201

Pressure-induced phase transitions in single-crystalline $Cu_4Bi_4S_9$ nanoribbons

Hu Jing-Yu, Li Jing, Zhang Si-Jia, Zhao Hao-Fei, Zhang Qing-Hua, Yao Yuan, Zhao Qing, Shi Li-Jie, Zou Bing-Suo, Li Yan-Chun, Li Xiao-Dong, Liu Jing, Zhu Ke, Liu Yu-Long, Jin Chang-Qing, Yu Ri-Cheng
Chin. Phys. B . 2013, 22(11): 116201. **doi:** 10.1088/1674-1056/22/11/116201

In situ electrical resistance and activation energy of solid C_{60} under high pressure

Yang Jie, Liu Cai-Long, Gao Chun-Xiao
Chin. Phys. B . 2013, 22(9): 096202. **doi:** 10.1088/1674-1056/22/9/096202

Pressure-induced enhancement of optoelectronic properties in PtS_2*

Yi-Fang Yuan(袁亦方)[1,2], Zhi-Tao Zhang(张志涛)[2], Wei-Ke Wang(王伟科)[3], Yong-Hui Zhou(周永惠)[2], Xu-Liang Chen(陈绪亮)[2], Chao An(安超)[2], Ran-Ran Zhang(张冉冉)[2], Ying Zhou(周颖)[2], Chuan-Chuan Gu(顾川川)[2], Liang Li(李亮)[4], Xin-Jian Li(李新建)[1,†], and Zhao-Rong Yang(杨昭荣)[2,5,‡]

[1] *Department of Physics and Laboratory of Material Physics, Zhengzhou University, Zhengzhou* 450052, *China*

[2] *Anhui Provincial Key Laboratory of Condensed Matter Physics at Extreme Conditions, High Magnetic Field Laboratory, Chinese Academy of Sciences, Hefei* 230031, *China*

[3] *Synergetic Innovation Center for Quantum Effects and Application, Key Laboratory of Low-dimensional Quantum Structures and Quantum Control of Ministry of Education, College of Physics and Information Science, Hunan Normal University, Changsha* 410081, *China*

[4] *State Key Laboratory of Material Processing and Die and Mould Technology, School of Materials Science and Engineering, Huazhong University of Science and Technology (HUST), Wuhan* 430074, *China*

[5] *Institute of Physical Science and Information Technology, Anhui University, Hefei* 230601, *China*

(Received 4 March 2018; revised manuscript received 14 April 2018; published online 30 May 2018)

PtS_2, which is one of the group-10 transition metal dichalcogenides, attracts increasing attention due to its extraordinary properties under external modulations as predicted by theory, such as tunable bandgap and indirect-to-direct gap transition under strain; however, these properties have not been verified experimentally. Here we report the first experimental exploration of its optoelectronic properties under external pressure. We find that the photocurrent is weakly pressure-dependent below 3 GPa but increases significantly in the pressure range of 3 GPa–4 GPa, with a maximum ~ 6 times higher than that at ambient pressure. X-ray diffraction data shows that no structural phase transition can be observed up to 26.8 GPa, which indicates a stable lattice structure of PtS_2 under high pressure. This is further supported by our Raman measurements with an observation of linear blue-shifts of the two Raman-active modes to 6.4 GPa. The pressure-enhanced photocurrent is related to the indirect-to-direct/quasi-direct bandgap transition under pressure, resembling the gap behavior under compression strain as predicted theoretically.

Keywords: high pressure, optoelectronic properties, transition metal disulfide

PACS: 62.50.–p, 85.60.–q, 32.30.Rj, 74.25.nd **DOI:** 10.1088/1674-1056/27/6/066201

1. Introduction

Transition metal dichalcogenides (TMDs), as a typical class of two-dimensional (2D) materials similar to graphene and black phosphorus, have attracted much attention because of their physical properties and promising potential applications in the field of electronics and optoelectronics.[1–7] Due to the quasi-2D nature of their lattice, they possess unique electronic band structure that can be effectively tuned by methods such as layer-dependence controlling, intercalating a variety of organic molecules, alkali or transition metals between the layered structures, applying pressure, mechanical strain or external electric fields on these materials.[6,8–18] For example, Mak *et al.* showed that decreasing the thickness of MoS_2 induces a crossover of the bandgap from indirect one in bulk material to a direct-gap in monolayer, which causes a strong enhancement of light emission as well as an increase of luminescence quantum efficiency by more than 4 orders of magnitude.[8] In addition, the intercalation of $C_3H_5NH_2$ molecules between layers of $NbSe_2$ behaves as electron donors and increases interlayer separations, resulting in profound changes in the electronic structure of the host lattice to induce an obvious increase of optical absorption.[11]

A computational study revealed that the electron mobilities of PtS_2 can be as high as ~ 4000 cm^2/V·s, which is among the highest in the selected TMDs.[4,5] Besides, PtS_2 has a large tunable bandgap, ranging from 1.6 eV in monolayer, 1.2 eV in the bilayer, and ultimately to 0.25 eV in the bulk PtS_2.[6] Recently, it was also shown that PtS_2 exhibits excellent optoelectronic performance with high responsivity up to 1.56×10^3 A/W and high detectivity of 2.9×10^{11} Jones.[9] Density functional theory (DFT) calculations predicted that, when under a mechanical strain, the indirect bandgap of monolayer PtS_2 becomes quasi-direct band-gap, which would be further in favor of the efficiency of light absorption and emission.[16]

In this paper, we employ high pressure means to manipulate the optoelectronic properties of PtS_2. Experimentally, it has been shown that the high pressure indeed plays an effective role in tuning the electronic properties of TMDs.[19–21] We find that the photocurrent shows weak pressure dependence below 3 GPa but increases rapidly until a maximum

*Project supported by the National Key Research and Development Program of China (Grant Nos. 2018YFA0305700 and 2016YFA0401804), the National Natural Science Foundation of China (Grant Nos. 11574323, 11704387, U1632275, 11304321, 11604340, and 61774136), the Natural Science Foundation of Anhui Province, China (Grant No. 1708085QA19), and the Director's Fund of Hefei Institutes of Physical Science, Chinese Academy of Sciences (Grant No. YZJJ201621).

†Corresponding author. E-mail: lixj@zzu.edu.cn

‡Corresponding author. E-mail: zryang@issp.ac.cn

© 2018 Chinese Physical Society and IOP Publishing Ltd

at ∼ 4 GPa, of ∼ 6 times higher than that at ambient pressure. Further increase of pressure results in a metallization and hence a sharp drop of photocurrent at 5.6 GPa–6 GPa. X-ray diffraction patterns reveal that the lattice structure of PtS_2 is ultra-stable under pressure, without observation of structural phase transition up to 26.8 GPa.

2. Experimental section

High-quality PtS_2 single crystals were grown by chemical vapor transport method using phosphorus as transporting agent.[9] The mixture of Pt, S, and P powers in stoichiometric ratio 1:3:1 was placed inside an evacuated and sealed quartz tube. The tube was slowly heated up to 85 °C on one end while the other end was kept at 75 °C. After 20 days of growth, plate-like crystals were obtained on the cold end. High-pressure photocurrent and resistance were performed in a screw-pressure-type diamond anvil cell made of BeCu alloy which was measured in High Magnetic Field Laboratory of the Chinese Academy of Sciences. Diamond anvils of 300-μm culets and a T301 stainless-steel gasket covered with a mixture of epoxy and fine cubic boron nitride (c-BN) powder were used for high-pressure transport measurements. The two-probe method was applied in the ab plane of single crystals with typical dimensions of 70 μm×40 μm×10 μm. The high-pressure photocurrent was measured under the illumination of a 532-nm excitation laser with power of 8.5 mW. The *in situ* high-pressure synchrotron radiation x-ray diffraction (XRD) ($\lambda = 0.3100$ Å) experiments were carried out at 16-BM-D station of High-Pressure Collaborative Access at Advanced Photo Source of Argonne National Laboratory.[22] The DIOPTAS and RIETICA programs were employed for the image integrations and the XRD profile refinements, respectively.[23,24] The LeBail method was used to extract the lattice parameters. High-pressure Raman scattering experiments were carried out using a Raman spectrometer with a 532-nm excitation laser. The ruby fluorescence method was used to determine the pressure for all of the above experiments.[25]

3. Results and discussion

A PtS_2-based device was fabricated for investigating the optoelectronic properties and transport properties under pressures. The sample configuration is illustrated in Fig. 1(a), where Au/Ti top electrodes were patterned via thermal evaporation. Figure 1(b) shows that all the *I*–*V* curves measured under different pressures exhibit linear behaviors, indicative of good Ohmic contacts between the sample and Au/Ti electrodes. Room-temperature electrical resistance was extracted from the slopes of the *I*–*V* curves and displayed as a function of applied pressure in Fig. 1(c). One can see that the resistance decreases monotonically with increasing pressure, which was well reproducible for compression and decompression procedures. The decrease of resistance under high pressure can be attributed to a gradually enhanced overlap of the electron wave functions during the compression of the lattice. When increasing the pressure to 6 GPa, the temperature-dependent resistance of PtS_2 device shows a metallic conduction behavior at 6 GPa, in contrast to that of the semiconducting behavior under ambient pressure condition as shown in Fig. 1(d).

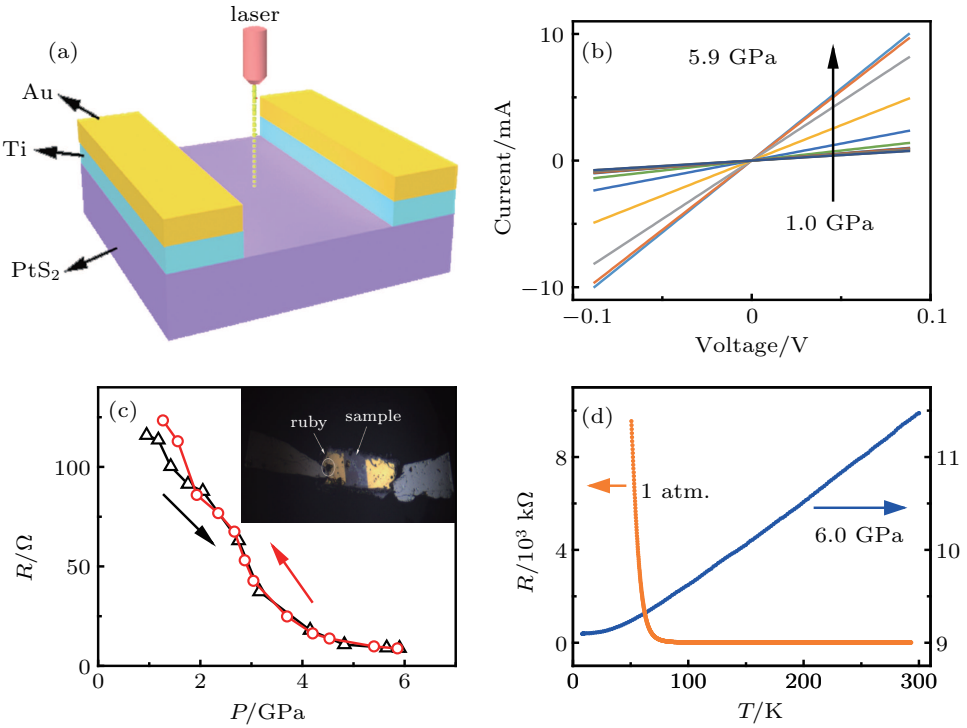


Fig. 1. (color online) (a) Schematic illustration of the structure of fabricated PtS_2 device. (b) The *I*–*V* curves of the PtS_2 device measured at room temperature under different applied pressures. (c) Pressure dependence of the room-temperature resistance of the PtS_2 device. Inset displays a microphotograph of the sample configuration in a DAC. (d) Temperature dependence of resistance measured under pressures of 1 atm (1 atm = 1.01325×10^5 Pa). and 6 GPa.

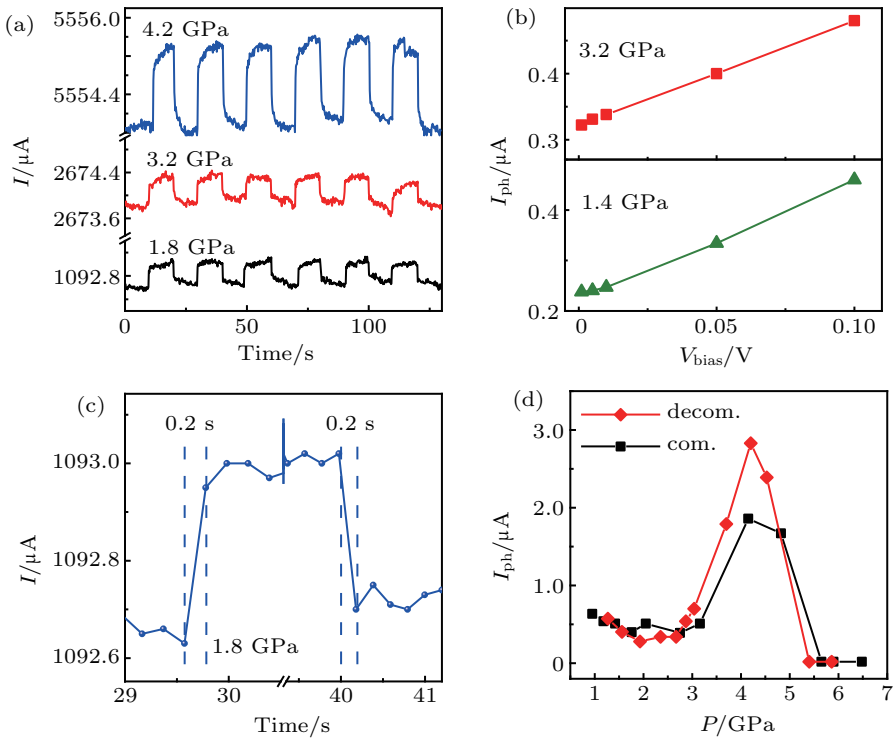


Fig. 2. (color online) (a) Photocurrent of the PtS_2 device measured under applied pressures of 1.8 GPa, 3.2 GPa, and 4.2 GPa. (b) The photocurrent as a function of bias-voltage under pressures of 1.4 GPa and 3.2 GPa. (c) Time-resolved photoresponse recorded at $V_{ds} = 0.1$ V. (d) The photocurrent as a function of applied pressure in compression (com.) and decompression (decom.) processes.

In order to examine the pressure effect on the optoelectronic properties of the PtS_2 device, we measured the time-dependent current *I*–*t* under different applied pressures, by intentionally switching ON/OFF the incident light of 532-nm laser illumination. The current was measured under a bias voltage of 0.1 V, in a linear range of $I(V_{bias})$ (see Fig. 2(b)). From Fig. 2(a), which displays the *I*–*t* curves under selected pressures, one can clearly see that the current *I* exhibits instant responses to the switching ON and OFF of the illumination. Zoom-in of a typical *I*–*t* pulse in Fig. 2(c) shows that the rise time and fall time, determined by the acquisition rate, are of ~ 0.2 seconds. This implies a real response time shorter than 0.2 seconds.

The values of photocurrent $I_{ph} = I_{illumination} - I_{dark}$ under different pressures are extracted from the *I*–*t* pulses and then represented as a function of applied pressure in Fig. 2(d). It is found that the photocurrent I_{ph} shows weak pressure dependence below 3 GPa and then increase with pressure rapidly until a maximum at around 4 GPa, where the I_{ph} is of ~ 6 times larger than that at ambient pressure. Further increase of the pressure results in a sharp drop of I_{ph}. We attribute such drop to the metallization of the system under high pressure, which is revealed by the pressure-dependent resistance measurements. The difference of I_{ph} between compression and decompression processes is ascribed to the hysteresis effect caused by the reduced pressure response of the lattice in decompression process, after the sample experienced an application of high pressure.

In some materials, such as ferroelectric photovoltaics $KBiFe_2O_5$, organic perovskite $CH_3NH_3PbBr_3$ and $CH_3NH_3SnI_3$, the variation of photoresponsivity ($R = I_{ph}/P_{eff}$, where P_{eff} is the effective illumination power) is originated from pressure-driven structural phase transition as revealed by existing literatures.[26–28] Therefore, it is of great interest to clarify what is happening to the lattice structure during the compression for understanding the change of the optoelectronic properties and resistance under pressure. The high-pressure *in situ* synchrotron x-ray diffraction (XRD) study of the PtS_2 sample was performed up to 26.8 GPa. Selected XRD spectra during compression procedures are displayed in Fig. 3(a). With increasing pressure in the whole measured range, no emergence of new diffraction peaks was observed, which excludes the possibility of occurrence of structural phase transition and indicates an ultra-stable lattice structure of PtS_2 under pressure up to 26.8 GPa.

The detailed lattice parameters were obtained by refinement of the XRD patterns using the Lebail method. The starting fitting point of structural parameters of the hexagonal (*P*-3*m*1) phase were taken from the study of PtS_2 by Furuseth *et al.*, and the fitted parameters were used for the starting point of the next higher-pressure point.[29] As an example, the lines at the bottom of Fig. 3(a) show the fitting results for 0.3 GPa with the *P*-3*m*1 space group ($a = b = 3.555$ Å, $c = 5.0188$ Å). The evolutions of the obtained lattice parameters with pressure are depicted in Figs. 3(b) and 3(c). It is found that the PtS_2 shows large anisotropy of axial compressibility: the *c* pa-

rameter decreases monotonically with increasing pressure by $\sim 22.7\%$ at 26.8 GPa, whereas the a parameter shows much weaker decrease of $\sim 1.7\%$. Such anisotropy, also given by the ratio of c/a, is due to the quasi 2D nature of the lattice structure. The pressure dependence of the cell volume is fitted to the third-order Birch–Murnaghan equation of state[30] (red line in Fig. 3(c)),

$$P(V) = \frac{3}{2}B_0\left[\left(\frac{V_0}{V}\right)^{7/3} - \left(\frac{V_0}{V}\right)^{5/3}\right] \times\left\{1+\frac{3}{4}(B_0'-4)\left[\left(\frac{V_0}{V}\right)^{2/3}-1\right]\right\},$$

where V, B, and B' are unit-cell volume at ambient condition, the ambient isothermal bulk modulus $-V/(\mathrm{d}V/\mathrm{d}P)$, and first order derivative of the bulk modulus at zero pressure, respectively. The obtained fitting results are $V = 55.01$ Å^3, $B = 43.61$ GPa, and $B' = 4.87$.

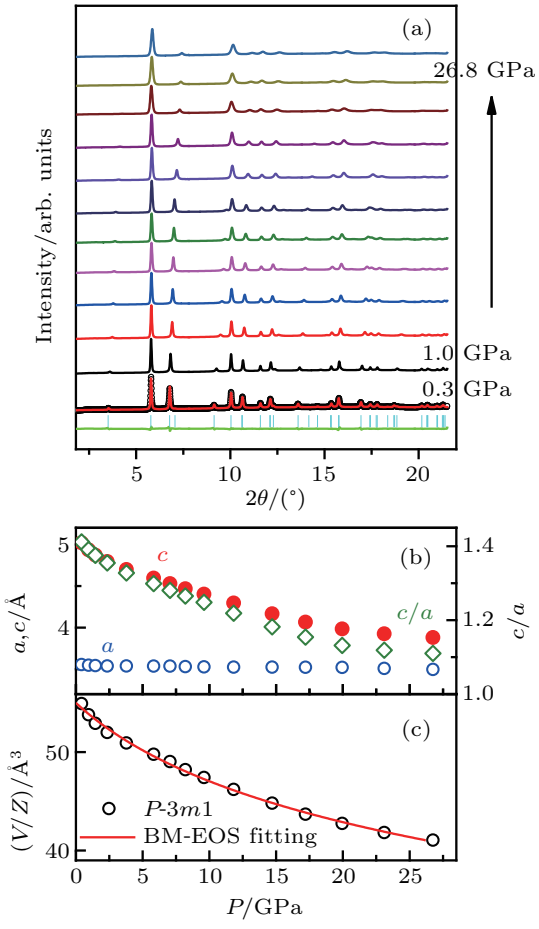


Fig. 3. (color online) (a) *in situ* high-pressure synchrotron x-ray diffraction (XRD) patterns of PtS_2 up to 26.8 GPa. As an example, the fitting of the 0.3-GPa XRD data is shown at the bottom, where experimental data in black circle, best fit in solid red curve, allowed reflections in blue tick marks, and the difference between the observed and calculated profiles in green curve (b). Pressure dependence of the lattice constants a, c, and $c = a$, as well as the cell volume in panel (c).

We further carried out a detailed Raman study on PtS_2 under pressures up to 6.4 GPa, to further confirm that the sharp increase of photocurrent between 3 GPa–4 GPa is NOT due to a potential structural phase transition. Figure 4(a) displays the *in situ* Raman spectra of PtS_2 during compression procedures. Consistent with previous report, two main Raman modes E_g and A_{1g} were observed at 309.4 cm^{-1} and 343.2 cm^{-1} under ambient pressure. As illustrated in the insets of Figs. 4(b) and 4(c), the out-of-plane A_{1g} mode occurs due to opposing vibrations of the two S atoms with respect to the Pt atom, and the E_g mode is associated with the in-plane-vibration of the two S atoms, in opposite direction with respect to each other.

With increasing pressure, the increase of relative intensity ratio of the E_g to A_{1g} peaks may be attributed to the dominance of the in-plane lattice vibration when the lattice is more strongly compressed along the c direction. The evolutions of the frequencies of the two modes are displayed as functions of pressure in Figs. 4(b) and 4(c). One can see that the frequencies of both E_g and A_{1g} peaks increase gradually with pressure. The continuous blue shifts of both peaks indicate the strengthened interaction between S and Pt atoms caused by the contraction of the lattice under pressure. In line with the XRD results, no abrupt anomaly is observed, which confirms the stability of the lattice under pressure below 6.4 GPa.

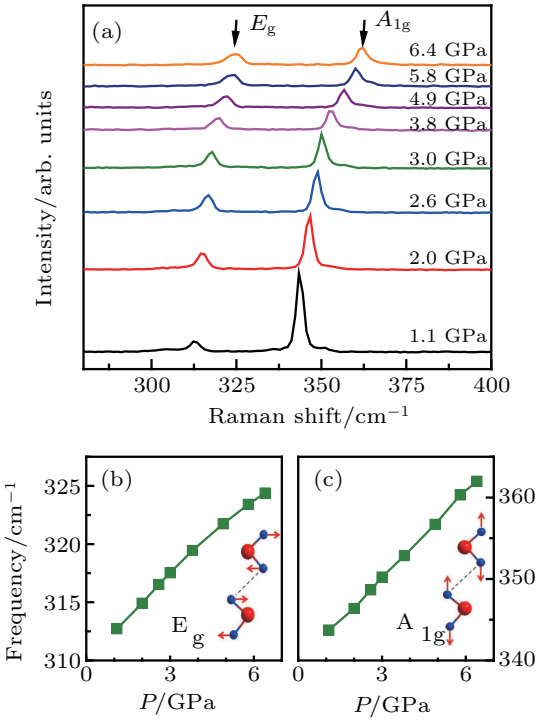


Fig. 4. (color online) (a) Raman spectra of PtS_2 under pressures up to 6.4 GPa in compression procedures. The peak frequencies of E_g and A_{1g} modes of PtS_2 as functions of applied pressure are displayed in panel (b) and panel (c), respectively. Insets of panels (b) and (c) depict the schematics of the E_g and A_{1g} vibration modes.

Generally, the ability of a semiconductor to absorb light and to gain photogenerated carriers is directly influenced by the band structure.[31] For a semiconductor with a direct bandgap, photons with energy higher than the bandgap are readily to be absorbed, but for a system with indirect bandgaps, the efficiency of absorption of photons is much

reduced due to the necessity of absorption of an additional phonon to supply the difference in momentum.[31] For example, benefiting from the direct nature of the bandgap in monolayer MoS_2 in contrast to the indirect bandgap in bulk MoS_2, the photoresponsivity (i.e., photocurrent per illumination power) of the monolayer MoS_2 was significantly enhanced by $\sim$ 9000 times compared to that in multilayer devices.[32] For monolayer PtS_2, as mentioned above, the density functional theory (DFT) calculations predict that a transition of the bandgap from an indirect nature to a quasi-direct one will take place when the system is under a mechanical strain,[16] which would be much in favor of the efficiency of light absorption and the yield of photogenerated carriers. Here in our PtS_2 device, we show that under high pressure of 1 GPa–3 GPa the resistance firstly decreases monotonically without obvious change of the photocurrent observed, indicative of a continuous narrowing of the indirect bandgap. But then in the pressure range of 3 GPa–4 GPa, the photocurrent displays a sharp increase with a maximum enhancement of $\sim$ 6 times compared to that at ambient pressure. These facts can be attributed to a underlying transition of the bandgap under pressure from an indirect gap to a direct or quasi-direct gap. Further increase of the pressure results in a metallization of the system (as is proved by our temperature-dependent resistance measurements) and hence a sharp drop of the photocurrent down to almost zero. All these results fit together and establish that the high pressure is an effective method to tune the band structure of PtS_2 and to improve the optoelectronic properties.

4. Conclusion

In summary, we report on the pressure-induced enhancement of optoelectronic properties in PtS_2. It is found that the photocurrent is effectively improved by $\sim$ 600% at $\sim$ 4 GPa compared to that at ambient pressure, which is attributed to an underlying bandgap transition from an indirect one to a direct or quasi-direct one. Further increase of the applied pressure causes a metallization of the system at 5.6 GPa–6 GPa. High-pressure XRD results indicate no structural phase transition and an ultra-stability of the lattice under pressures up to 26.8 GPa. Our results reveal that pressure is a simple but effective tool to improve the optoelectronic properties of PtS_2.

Acknowledgment

The x-ray work was performed at HPCAT (Sector 16), Advanced Photon Source, Argonne National Laboratory. HPCAT operations were supported by DOE-NNSA under Award No. DE-NA0001974 and DOE-BES under Award No. DE-FG02-99ER45775, with partial instrumentation funding by NSF. The Advanced Photon Source is a US Department of Energy (DOE) Office of Science User Facility operated for the DOE Office of Science by Argonne National Laboratory under Contract No. DE-AC02-06CH11357.

References

[1] Mak K F and Shan J 2016 *Nat. Photon.* **10** 216
[2] Li L K, Kim j, Jin C H, Ye G J, Qiu D Y, da Jornada F H, Shi Z W, Chen L, Zhang Z C, Yang F Y, Watanabe K, Taniguchi T, Ren W C, Louie S G, Chen X H, Zhang Y B and Wang F 2016 *Nat. Nanotechnol.* **12** 21
[3] Joshua O I, Gary A S, Herre S J v d Z and Andres C G 2015 *2D Mater.* **2** 011002
[4] Bao W Z, Cai X H, Kim D, Sridhara K and Fuhrer M S 2013 *Appl. Phys. Lett.* **102** 042104
[5] Huang Z S, Zhang W X and Zhang W L 2016 *Materials* **9** 716
[6] Zhao Y D, Qiao J S, Yu P, Hu Z X, Lin Z Y, Lau S P, Liu Z, Ji W and Chai Y 2016 *Adv. Mater.* **28** 2399
[7] Wang W K, Li L, Zhang Z T, Yang J Y, Tang D S and Zhai T Y 2017 *Appl. Phys. Lett.* **111** 203504
[8] Mak K F, Lee C G, Hone J, Shan J and Heinz T F 2010 *Phys. Rev. Lett.* **105** 136805
[9] Li L, Wang W K, Chai Y, Li H Q, Tian M L and Zhai T Y 2017 *Adv. Funct. Mater.* 1701011
[10] Zhang Y, ChangT R, Zhou B, Cui Y T, Yan H, Liu Z K, Schmitt F, Lee J, Moore R, Chen Y L, Lin H, Jeng H T, Mo S K, Hussain Z, Bansil A and Shen Z X 2013 *Nat. Nanotechnol.* **9** 111
[11] Friend R H and Yoffe A D 1987 *Adv. Phys.* **36** 1
[12] Benavente E, Santa Ana M A, Mendizábal F and González G 2002 *Coord. Chem. Rev.* **224** 87
[13] Mann J, Ma Q, Odenthal P M, Isarraraz M, Le D, Preciado E, Barroso D, Yamaguchi K, von Son Palacio G, Nguyen A, Tran T, Wurch M, Nguyen A, Klee V, Bobek S, Sun D, Heinz T F, Rahman T S, Kawakami R and Bartels L 2014 *Adv. Mater.* **26** 1399
[14] Chhowalla M, Shin H S, Eda G, Li L J, Loh K P and Zhang H 2013 *Nat. Chem.* **5** 263
[15] Conley H J, Wang B, Ziegler J I, Haglund R F, Pantelides S T and Bolotin K I 2013 *Nano Lett.* **13** 3626
[16] Miró P, Ghorbani-Asl M and Heine T 2014 *Angew. Chem. Int. Ed.* **53** 3015
[17] Zhao Z, Zhang H J, Yuan H T, Wang S B, Lin Y, Zeng Q S, Xu G, Liu Z X, Solanki G K, Patel K D, Cui Y, Hwang H Y and Mao W L 2015 *Nat. Commun.* **6** 7312
[18] Ramasubramaniam A, Naveh D and Towe E 2011 *Phys. Rev. B* **84** 205325
[19] Nayak A P, Bhattacharyya S, Zhu J, Liu J, Wu X, Pandey T, Jin C Q, Singh A K, Akinwande D and Lin J F 2014 *Nat. Commun.* **5** 3731
[20] Wang X F, Chen X L, Zhou Y H, Park C Y, An C, Zhou Y, Zhang R R, Gu C C, Yang W G and Yang Z R 2017 *Sci. Rep.* **7** 46694
[21] Zhou D W, Zhou Y H, Pu C Y, Chen X L, Lu P C, Wang X F, An C, Zhou Y, Miao F, Ho C H, Sun J, Yang Z R, Xing D Y 2017 *npj Quantum Materials* **2**
[22] Park C Y, Popov D, Ikuta D, Lin C L, Kenney-Benson C, Rod E, Bommannavar A and Shen G Y 2015 *Rev. Sci. Instrum.* **86** 072205
[23] Prescher C and Prakapenka V B 2015 *High Pressure Research* **35** 223
[24] Hunter B A 1998 Rietica-A Visual Rietveld Program, International Union of Crystallography Commission on Powder Diffraction Newsletter No. 20 (Summer 1998) http://www.rietica.org
[25] Mao H K, Xu J and Bell P M 1986 *J. Geophys. Res.-Sol. Ea.* **91** 4673
[26] Wang Y G, Lü X J, Yang W G, Wen T, Yang L X, Ren X T, Wang L, Lin Z S and Zhao Y S 2015 *J. Am. Chem. Soc.* **137** 11144
[27] Lü X J, Wang Y G, Stoumpos C C, Hu Q Y, Guo X F, Chen H J, Yang L X, Smith J S, Yang W G, Zhao Y S, Xu H W, Kanatzidis M G and Jia Q X 2016 *Adv. Mater.* **28** 8663
[28] Zhang G H, Liu F L, Gu T T, Zhao Y S, Li N N, Yang W G and Feng S H 2017 *Adv. Electron. Mater.* **3** 1600498
[29] Furuseth S, Selte K and Kjekshus A 1965 *Acta Chem. Scand.* **19** 257
[30] Birch F 1947 *Phys. Rev.* **71** 809
[31] Wang Q H, Kalantar-Zadeh K, Kis A, Coleman J N and Strano M S 2012 *Nat. Nanotechnol.* **7** 699
[32] Lopez-Sanchez O, Lembke D, Kayci M, Radenovic A and Kis A 2013 *Nat. Nanotechnol.* **8** 497